

Benchmarking Polarizable Molecular Dynamics Simulations of Aqueous Sodium Hydroxide by Diffraction Measurements[†]

Robert Vácha,[‡] Tunde Megyes,[§] Imre Bakó,[§] László Pusztai,^{||} and Pavel Jungwirth^{*‡}

Institute of Organic Chemistry and Biochemistry, Academy of Sciences of the Czech Republic and Center for Biomolecules and Complex Molecular Systems, Flemingovo nám. 2, 16610 Prague 6, Czech Republic, Institute of Structural Chemistry, Chemical Research Center of the Hungarian Academy of Sciences, Pusztaszeri út 59-67, H-1025 Budapest, Hungary, and Research Institute for Solid State Physics and Optics, Hungarian Academy of Sciences, H-1525 Budapest, P.O. Box 49, Hungary

Received: November 26, 2008; Revised Manuscript Received: January 8, 2009

Results from molecular dynamics simulations of aqueous hydroxide of varying concentrations have been compared with experimental structural data. First, the polarizable POL3 model was verified against neutron scattering using a reverse Monte Carlo fitting procedure. It was found to be competitive with other simple water models and well suited for combining with hydroxide ions. Second, a set of four polarizable models of OH⁻ were developed by fitting against accurate ab initio calculations for small hydroxide–water clusters. All of these models were found to provide similar results that robustly agree with structural data from X-ray scattering. The present force field thus represents a significant improvement over previously tested nonpolarizable potentials. Although it cannot in principle capture proton hopping and can only approximately describe the charge delocalization within the immediate solvent shell around OH⁻, it provides structural data that are almost entirely consistent with data obtained from scattering experiments.

Introduction

A key element in the validation of computer simulation results is the comparison with experimental data. Structural quantities, which are typically the most suitable ones for the purpose, are frequently calculated from molecular dynamics (MD) and Monte Carlo (MC) simulations and then contrasted with their experimental counterparts.¹ It is the radial distribution function (rdf or $g(r)$) that is most often used for comparison, even though the rdf is not a direct result of diffraction experiments. This is the reason why it is advisable to consider the primary experimental outcome, the total scattering structure factor (tssf or $F(Q)$), wherever possible as well. A scheme based on the reverse Monte Carlo (RMC) procedure² provides a bridge between diffraction experiments and interaction potential models.³

A common element of the simulation of aqueous solutions is the use of a particular potential model of water, the applicability of which should be established. A polarizable three-site POL3 potential⁴ has been employed in our previous studies of aqueous interfaces as a reasonable compromise between simplicity and accuracy, and it is this model that is being scrutinized from the structural point of view in the present study. Pure water, the simplest system considered in this work, can be investigated in great detail. Therefore, the primary source of experimental information on the structure, that is, the tssf, is used for validation purposes in the procedure,³ which offers a direct consistency check between experimental data and the potential model. In the next step, results from experiment and simulations are compared for a more complex system, the

TABLE 1: Oxygen Parameters for the Four Employed Potential Models for Hydroxide^a

	q [e]	σ [nm]	ϵ [kJ/mol]
M1	-1.35	0.373	0.652704
M2	-1.35	0.384	0.4184
M3	-1.35	0.367	0.8368
M4	-1.20	0.384	0.652704

^a There are no Lennard-Jones parameters on the hydroxide hydrogen, the charge of which is deduced from that on the oxygen and from the overall $-1e$ charge of the ion.

aqueous solution of NaOH.⁵ Here the most robust means of comparison as applied to pure water could not yet be applied, although work toward the realization of such a scheme for NaOH solutions is underway. Therefore, here we restrict ourselves to comparisons at the level of rdf's.

The principal motivation behind the present study of NaOH(aq) is the interfacial behavior of hydroxide anion, which has been a subject of a recent controversy.^{6–8} Simulations, spectroscopic experiments, and surface tension measurements indicate no, or at best, weak, surface affinity of OH⁻.^{9–13} In contrast, results of ζ potential and titration measurements on air bubbles and oil droplets in water are interpreted in terms of a very strong surface adsorption of hydroxide.^{14–16} Whereas potentials employed in these simulations have been tested against ab initio calculations, here we compare directly with the experiment.

Methods

Molecular Dynamics Simulations. We developed and tested four different force fields for OH⁻. All models had the same geometry with the O–H distance of 1 Å and polarizability of 2.1 Å³ placed at the oxygen atom.¹⁷ The remaining parameters, presented in Table 1, were optimized against ab initio MP2/

[†] Part of the special issue “George C. Schatz Festschrift”.

* Corresponding author. E-mail: pavel.jungwirth@uochb.cas.cz.

[‡] Academy of Sciences of the Czech Republic and Center for Biomolecules and Complex Molecular Systems.

[§] Chemical Research Center of the Hungarian Academy of Sciences.

^{||} Research Institute for Solid State Physics and Optics, Hungarian Academy of Sciences.

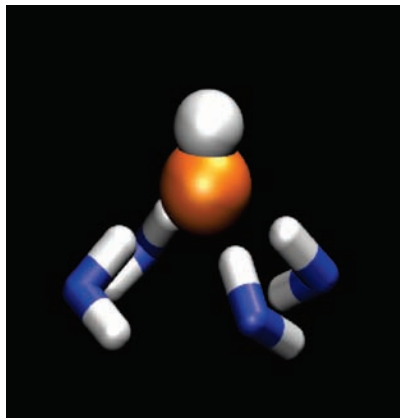


Figure 1. Geometry of the ab initio local minimum of a cluster containing OH^- and four water molecules used for optimizing the polarizable potentials.

aug-cc-pVDZ interaction energies of OH^- with the four most strongly interacting water molecules calculated with the program package Gaussian 03.¹⁸ (For the employed local minimum geometry, see Figure 1.) The first force-field model, which adopted a charge distribution from the natural population analysis, was taken from our previous paper¹⁷ and is referred to as M1. The next two models have modified Lennard-Jones terms on oxygen. Additionally, the last model has a modified charge distribution and, consequently, the permanent dipole. Here the partial charges were calculated using the RESP method after ab initio Hartree–Fock calculation in the 6-31g* basis via fitting the electrostatic potential at points selected according to the Merz–Singh–Kollman scheme. After matching the force field and ab initio interaction energies for the $\text{OH}^-(\text{H}_2\text{O})_4$ cluster for all four models, these were then also checked for an optimal cluster of hydroxide and three water molecules. The agreement with MP2/aug-cc-pVDZ was excellent for all models. Note that for water, we employed the polarizable POL3 model,⁴ and for the water–hydroxide Lennard-Jones potential, we used standard combination rules (i.e., arithmetic mean for σ and geometric mean for ϵ).

All of our MD simulations were performed using the program package Gromacs version 3.3.1 compiled in double precision.¹⁹ A time step of 1 fs was used with a cutoff of 1.1 nm for nonbonded interactions. Long-range electrostatic interactions were treated using the particle mesh Ewald (PME) method.²⁰ The systems were simulated in the NPT ensemble with Berendsen temperature and pressure coupling²¹ set at 300 K and 1 atm. We modeled systems with four particular compositions: pure water and 1, 2.4, and 4.8 M solutions of NaOH, each containing about 700 water molecules and the corresponding number (for the particular concentration) of Na^+ and OH^- ions.

Reverse Monte Carlo. To compare simulation results for the POL3 water model with experimental structural data, we have applied a novel approach³ that combines experimentally determined tssf's and partial radial distribution functions from MD simulations into a single structural model. Such particle configurations may be constructed by the RMC method.^{22–24} We require agreement within experimental uncertainties with diffraction data and at the same time inquire how well the potential-based partial radial distribution functions (prdf's) can be reproduced. In this way, it is possible to tell if (or which of) the simulated partial radial distribution functions are consistent with the experimental tssf's. Note that this approach, while also being more instructive, is easier to perform than combining

prdf's from MD simulations to provide the tssf's. This is because the size of the simulation box is not important since no Fourier transform is carried out and there is no difficulty with rigid water models, for which approximations concerning the intramolecular part would otherwise be necessary.²⁵

In the RMC calculations, 2000 flexible water molecules (i.e., 6000 atoms) were employed at the experimental atomic number density of 0.099 atoms per \AA^{-3} . According to the protocol described in ref 3, the experimental tssf of heavy water²⁶ along with the three (O–O, O–H, and H–H) prdf's from an MD simulation of bulk POL3 water⁴ were used as input data for RMC.

Very recently, a comparison using a similar protocol of several water potentials including the POL3 model was performed by one of us.²⁷ In that work, the very same conditions for each potential model had to be used to facilitate unbiased comparison. As a result of such analysis, the POL3 model performed well in terms of the overall fit; nevertheless, consistency with the experimental data set was not optimal without weighting input prdf's. The level of consistency between diffraction experiments and the POL3 water model is improved in this study through systematic optimization of weights of the input data sets while keeping the experimental tssf within experimental uncertainties and having the best possible fit to prdf's from the MD simulations. To find the most appropriate parameters as well as the finest balance between experiment and the POL3 potential model (via the corresponding simulated prdf's), about 10 RMC calculations had to be carried out, of which only the best one is reported here.

Experiments: Structure Factors of Pure Water. Because the tssf ($F(Q)$) has a central role in assessing the quality of the water potential, it is helpful to recall that (focusing here on results from neutron diffraction experiments) it is defined as²⁸

$$G(r) = \sum_{i,j=1}^n c_i c_j \bar{b}_i \bar{b}_j [g_{ij}(r) - 1] \quad (1a)$$

$$F(Q) = \rho_0 \int_0^\infty 4\pi r^2 G(r) \frac{\sin Qr}{Qr} dr \quad (1b)$$

In eqs 1a and 1b, c_i and b_i are the molar ratio and the scattering length of species i , $g_{ij}(r)$ are the prdf's, $G(r)$ is the total rdf, ρ_0 is the number density, and Q is the scattering variable (proportional to the scattering angle); indexes i and j run through nuclear species of the system.

The experimental input information, that is, the tssf for pure heavy water (D_2O) under ambient conditions has been obtained from neutron diffraction experiments conducted at a pulsed neutron source (ISIS Facility, U.K.).²⁶ The neutron scattering amplitudes (the so-called coherent scattering lengths, b) of the deuteron and the oxygen atom are 6.7 and 5.8 fm. Taking into account molar ratios of H and O, this yields the appropriate weighting factors of the O–O, O–H, and H–H pair correlations of 0.09, 0.42, and 0.49. Neutron diffraction is a convenient tool for the present measurements because the scattering lengths are independent of Q (and of the scattering angle). Also, the above weighting factors are valid for both Q -space (tssf) and r -space (rdf) data.

Experiments: Sodium Hydroxide Solutions. 1.0, 2.5, and 4.8 M samples of aqueous NaOH were measured for the direct comparison with the simulated systems. X-ray scattering measurements were performed at room temperature (24 ± 1 °C), with a Philips X'Pert goniometer in a vertical Bragg–Brentano geometry with a pyrographite monochromator in the scattered beam using Mo $K\alpha$ radiation ($\lambda = 0.7107$ Å). The liquid sample

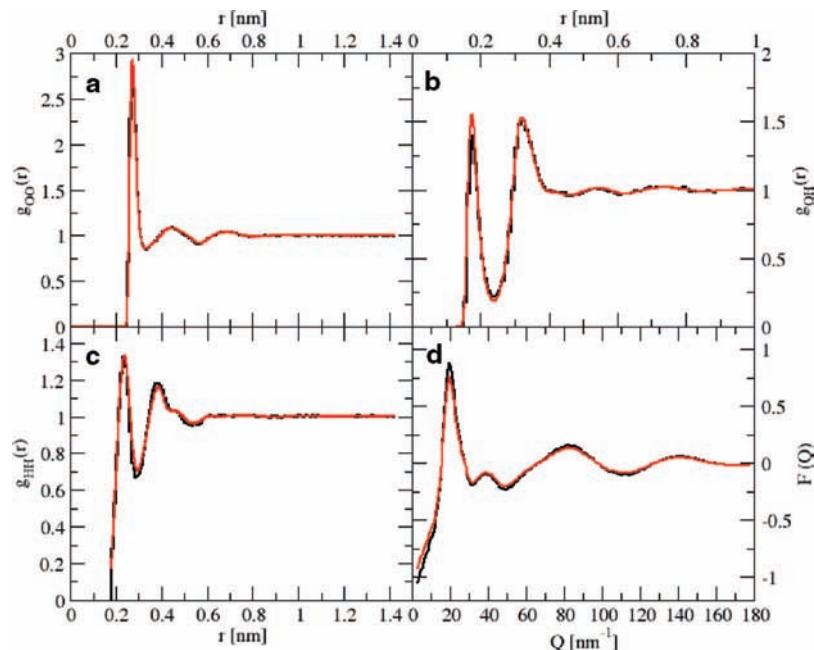


Figure 2. RMC modeling of the (a) O–O, (b) O–H, and (c) H–H partial radial distribution functions from the MD simulation of bulk water using the POL3 water potential⁴ and neutron diffraction experimental data on pure heavy water.²⁶ For a–c, black lines represent input partial rdf's from MD simulations and red lines represent RMC. For d, the black line represents the experimental total scattering structure factor and the red line represents RMC.

holder had plane–parallel windows prepared from 75 μm thin foils of bioriented polypropylene. The scattering angle range of measurement spanned over $1.28^\circ \leq 2\Theta \leq 120^\circ$ corresponding to a range of $0.2 \text{ \AA}^{-1} \leq k \leq 15.3 \text{ \AA}^{-1}$ of the scattering variable $k = (4\pi/\lambda) \sin \Theta$. Over 100 000 counts were collected by a proportional detector at each of the 150 discrete angles selected in $\Delta k \approx 0.1 \text{ \AA}^{-1}$ steps in several repeated runs (10 000 counts at each point). The measurement technique and data treatment were essentially the same as those in our previous study.²⁹

Results

Water Structure: Experiment and Simulation. The best results obtained by applying the RMC fitting scheme of ref 3 to the POL3 water potential are summarized in Figure 2. It follows from this Figure that the consistency with experimental data is very good. In other words, by using the POL3 water model, it was possible to obtain a fit that was almost within the experimental error. Nevertheless, full consistency with neutron diffraction data on liquid D₂O (i.e., indistinguishable curves for experimental data and the fit) was not reached for small sections of pdf's of POL3 water. More precisely, it is the O–O pdf that may be termed entirely consistent with available diffraction data, whereas the O–H and H–H pdf's display small deviations. We note that further attempts to improve the quality of the fits to these functions lead to the deterioration of the level of consistency with experimental data, which again indicates small inconsistencies between diffraction data and the potential model in question.

Sodium Hydroxide Solutions: Computational Results. The hydroxide oxygen–water hydrogen (O–HW) pdf's and integrals thereof (i.e., cumulative sums) are presented in Figure 3 for the four potential models employed. The profiles of pdf's are very similar to each other, with the main difference being a small shift in the first peak corresponding to slightly different sizes of the hydroxide oxygens in different force fields. The oxygen atom of hydroxide has four to five water hydrogens in

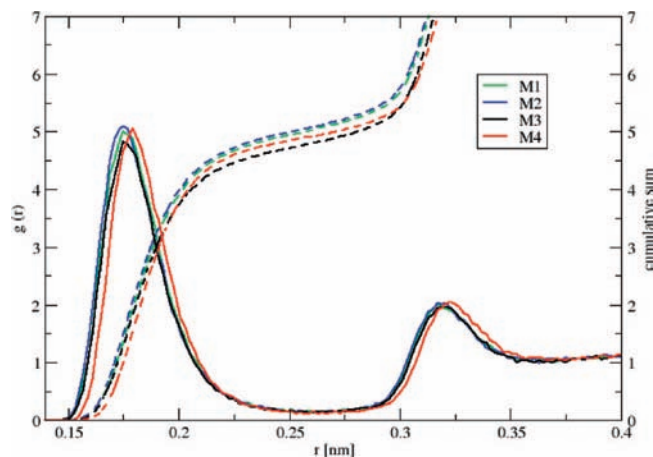


Figure 3. Partial radial distribution functions (—) and corresponding cumulative sums (---) for hydroxide oxygen and water hydrogen in 1 M solution of NaOH using the four different models of OH[−].

the first solvation shell for all models (Figure 3). Note that the second peak in Figure 3 corresponds to the outer shell of water molecules around OH[−] including that weakly hydrogen bonded to the hydrogen of hydroxide.^{5,30,31} M2 and M4 turned out to be the most distinct among the four investigated models; therefore, they were employed in further studies of 1, 2.4, and 4.8 M NaOH solutions.

For all of the above concentrations, we calculated pdf's resulting from the M2 and M4 models, as depicted in Figure 4. Although the two models perform similarly, sodium ions interact more strongly with hydroxide and water oxygens (having a higher first peak) within the M4 model compared with the M2 model, with the location of the first maximum being shifted to slightly larger distances. For the distribution of water oxygens around hydroxide oxygens, we see a small effect of the slightly larger hydroxide oxygen within the M4 model; otherwise, the two potentials perform similarly. There is no visible effect of a particular OH[−] model on rdf's between Na⁺ and water oxygens

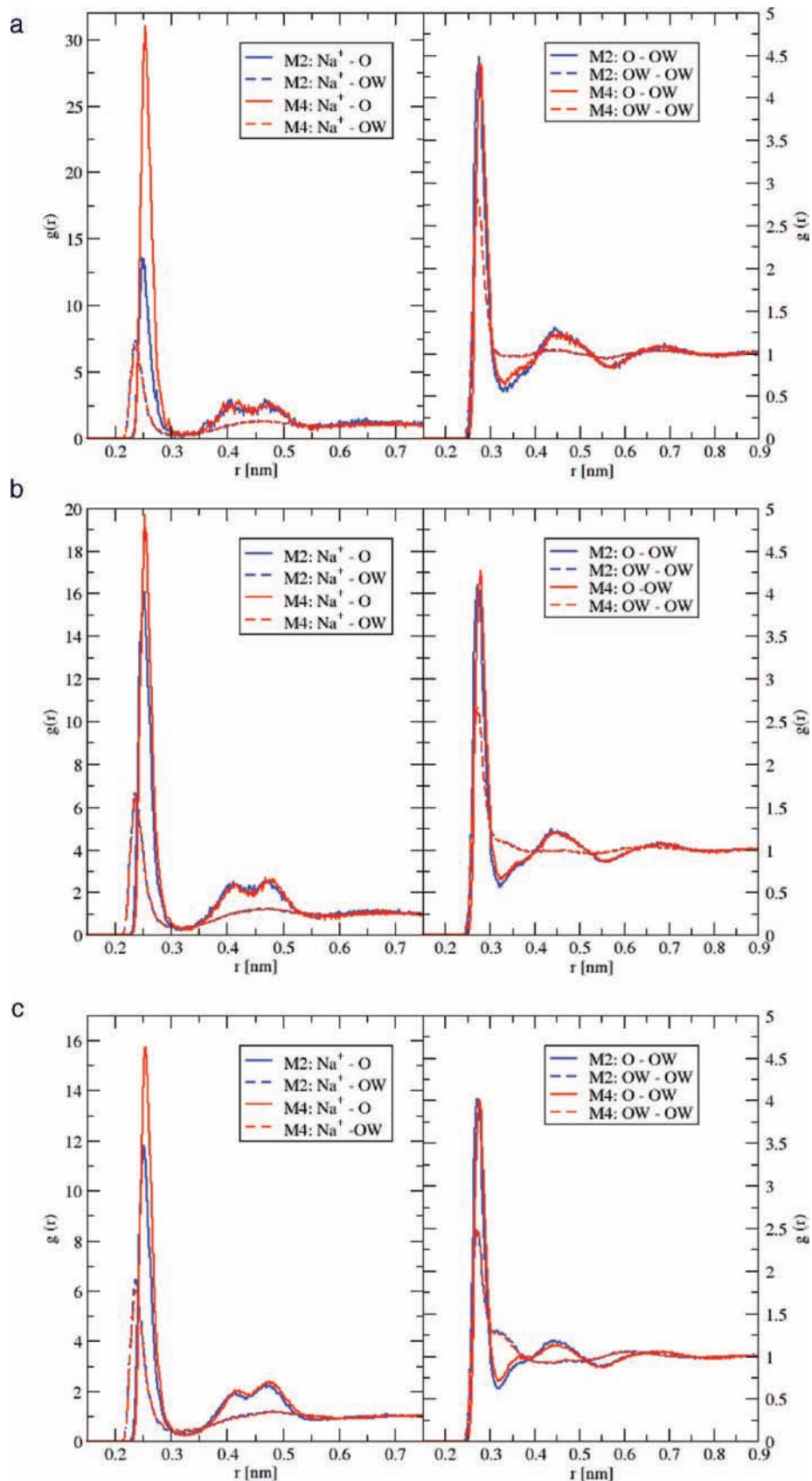


Figure 4. Partial radial distribution functions for sodium (Na^+) and oxygens on hydroxide (O) and water (OW) at: (a) 1, (b) 2.4, and (c) 4.8 M NaOH solution. The model M2 is plotted in blue, whereas the model M4 is plotted in red.

(OW) and on the OW - OW distribution for any of the studied concentrations. Such a result is not unexpected because this is a second-order effect of the hydroxide potential.

In summary, the differences among the investigated models of hydroxide are small. The simulation results are, therefore, robust.

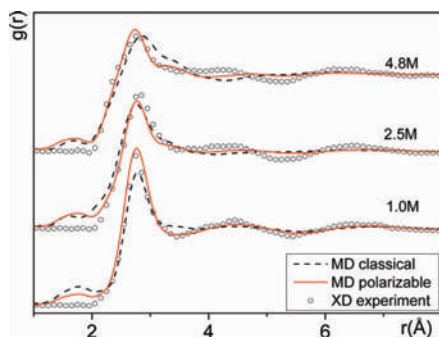


Figure 5. Comparison of total radial distribution functions obtained from the experiment (○) and from MD simulations using a nonpolarizable model (black line) and a polarizable model (red line).

Sodium Hydroxide Solutions: Experimental Results. The rdf's obtained from X-ray diffraction experiments are compared with simulated ones in Figure 5. The part of the total structure function that is relevant to the liquid structure (i.e., that without intramolecular contribution) can be calculated from the prdf's according to the equation

$$H(k) = \sum_{\alpha \geq \beta} \sum_{\alpha \neq \beta} \frac{(2 - \delta_{\alpha\beta})x_{\alpha}x_{\beta}f_{\alpha}f_{\beta}h_{\alpha\beta}(k)}{M(k)} \quad (2)$$

Here f_{α} is the scattering length or scattering factor of the α -notated atom (which depends on k in the case of X-ray diffraction) and x_{α} is the corresponding mole fraction. $h_{\alpha\beta}(k)$ is defined according to the following equation

$$h_{\alpha\beta}(k) = 4\pi\rho \int_0^{r_{\max}} r^2 (g_{\alpha\beta}(r) - 1) \frac{\sin(kr)}{kr} dr \quad (3)$$

The total rdf is then given as the Fourier transform of the structure function.

As described in ref 29, classical nonpolarizable potentials cannot appropriately describe the interaction between water and hydroxide anion. The agreement between experiment and simulations employing either of the present polarizable potentials is significantly better (Figure 5). From the experimental point of view, the M2 and M4 polarizable potential models are indistinguishable.

Discussion and Conclusions

To validate polarizable force fields for aqueous hydroxide solutions, it is imperative to check the employed water model first. The comparison with neutron scattering results shows that from the point of view of the static structure, the POL3 potential model of liquid water is certainly competitive in comparison with other commonly used water potentials considered recently.²⁷ In this work, it is demonstrated that the already quite favorable level of consistency with experiment reported in ref 27 can be further improved using the RMC procedure. That is, from the structural point of view, the POL3 water model represents an appropriate choice for the purpose of simulating ambient liquid water properties despite its possible shortcomings in accurately describing the full phase diagram of water. In the ambient liquid, the description of the O–O correlation function is excellent, whereas there are small discrepancies for the O–H and H–H pair correlation functions (Figure 2). For the latter prdf's, quantum nuclear effects, which are not considered or are at best only implicitly accounted for in the present classical simulations, may come into play.

Having validated the water force field, we proceeded with testing four polarizable models for hydroxide. All of these

models are constructed in a similar way differing somewhat in the values of oxygen Lennard-Jones parameters, the partial charges, or both. They are fitted against accurate ab initio calculations on small hydroxide–water clusters, which also makes them consistent with the employed POL3 water model. These four OH[−] models provide aqueous structural data that are very similar to each other and are in a semiquantitative agreement with the prdf's obtained from X-ray data. The present models thus represent a major improvement over a nonpolarizable force field previously employed in the comparison with structural data.²⁹ Clearly, classical MD simulations cannot describe proton hopping and can only partially capture fine structural subtleties connected to the partial charge delocalization of hydroxide over the water solvation shell.^{5,32} Nevertheless, structural features of the present polarizable model of aqueous hydroxide are in good agreement with experiment despite the relative simplicity (and, consequently, computational efficiency) of the employed force field.

Acknowledgment. P.J. acknowledges support from the Czech Ministry of Education (grant LC512) and via the project Z40550506. R.V. acknowledges support from the Czech Science Foundation (grant 203/05/H001) and from the International Max Planck Research School. L.P. acknowledges financial help from the Hungarian Basic Research Fund (OTKA) via grant no. T048580. I.B. acknowledges financial help from the Hungarian Basic Research Funds (OTKA) via project no. K 68140. T.M. acknowledges the support from project NAP VENEUS05 OMF06-00650/2005.

References and Notes

- (1) Allen, M. P.; Tildesley, D. J. *Computer Simulations of Liquids*; Oxford: Clarendon, 1987.
- (2) McGreevy, R. L.; Pusztai, L. Reverse Monte Carlo simulation: a new technique for the determination of disordered structures. *Mol. Simul.* **1988**, *1*, 359.
- (3) Pusztai, L.; Harsanyi, I.; Dominguez, H.; Pizio, O. Assessing the level of consistency between diffraction experiments and interaction potentials: a combined molecular dynamics (MD) and Reverse Monte Carlo (RMC) approach. *Chem. Phys. Lett.* **2008**, *457*, 96–102.
- (4) Caldwell, J. W.; Kollman, P. A. Structure and properties of neat liquids using nonadditive molecular dynamics: water, methanol, and *N*-methylacetamide. *J. Phys. Chem.* **1995**, *99*, 6208–6219.
- (5) Tuckerman, M. E.; Chandra, A.; Marx, D. Structure and dynamics of OH-(aq). *Acc. Chem. Res.* **2006**, *39*, 151–158.
- (6) Vácha, R.; Buch, V.; Milet, A.; Devlin, P.; Jungwirth, P. Autoionization at the surface of neat water: is the top layer pH neutral, basic, or acidic? *Phys. Chem. Chem. Phys.* **2007**, *9*, 4736–4747.
- (7) Beattie, J. K. Comment on autoionization at the surface of neat water: is the top layer pH neutral, basic, or acidic? by R. Vácha, V. Buch, A. Milet, J. P. Devlin and P. Jungwirth. *Phys. Chem. Chem. Phys.*, **2007**, *9*, 4736. *Phys. Chem. Chem. Phys.* **2008**, *10*, 330–331.
- (8) Vácha, R.; Buch, V.; Milet, A.; Devlin, J. P.; Jungwirth, P. Response to comment on autoionization at the surface of neat water: is the top layer pH neutral, basic, or acidic? by J. K. Beattie. *Phys. Chem. Chem. Phys.*, **2007**, *9*, DOI: 10.1039/b713702h. *Phys. Chem. Chem. Phys.* **2008**, *10*, 332–333.
- (9) Buch, V.; Milet, A.; Vácha, R.; Jungwirth, P.; Devlin, J. P. Water surface is acidic. *Proc. Natl. Acad. Sci. U.S.A.* **2007**, *104*, 7342–7347.
- (10) Petersen, P. B.; Saykally, R. J. Is the liquid water surface basic or acidic? Macroscopic vs molecular-scale investigations. *Chem. Phys. Lett.* **2008**, *458*, 255–261.
- (11) Mucha, M.; Frigato, T.; Levering, L. M.; Allen, H. C.; Tobias, D. J.; Dang, L. X.; Jungwirth, P. Unified molecular picture of the surfaces of aqueous acid, base, and salt solutions. *J. Phys. Chem. B* **2005**, *109*, 7617–7623.
- (12) Tarbuck, T. L.; Ota, S. T.; Richmond, G. L. Spectroscopic studies of solvated hydrogen and hydroxide ions at aqueous surfaces. *J. Am. Chem. Soc.* **2006**, *128*, 14519–14527.
- (13) Tian, C. S.; Ji, N.; Waychunas, G. A.; Shen, Y. R. Interfacial structures of acidic and basic aqueous solutions. *J. Am. Chem. Soc.* **2008**, *130*, 13033–13039.
- (14) Beattie, J. K. The intrinsic charge on hydrophobic microfluidic substrates. *Lab Chip* **2006**, *6*, 1409–1411.

- (15) Beattie, J. K.; Djerdjev, A. M. The pristine oil/water interface: surfactant-free hydroxide-charged emulsions. *Angew. Chem., Int. Ed.* **2004**, *43*, 3568–3571.
- (16) Marinova, K. G.; Alargova, R. G.; Denkov, N. D.; Velev, O. D.; Petsev, D. N.; Ivanov, I. B.; Borwankar, R. P. Charging of oil–water interfaces due to spontaneous adsorption of hydroxyl ions. *Langmuir* **1996**, *12*, 2045–2051.
- (17) Vácha, R.; Horinek, D.; Berkowitz, M. L.; Jungwirth, P. Hydronium and hydroxide at the interface between water and hydrophobic media. *Phys. Chem. Chem. Phys.* **2008**, *10*, 4975–4980.
- (18) Frisch, M. J.; Trucks, G. W.; Schlegel, H. B.; Scuseria, G. E.; Robb, M. A.; Cheeseman, J. R.; Montgomery J.A. Jr.; Vreven, T.; Kudin, K. N.; Burant, J. C.; Millam, J. M.; Iyengar, S. S.; Tomasi, J.; Barone, V.; Mennucci, B.; Cossi, M.; Scalmani, G.; Rega, N.; Petersson, G. A.; Nakatsuji, H.; Hada, M.; Ehara, M.; Toyota, K.; Fukuda, R.; Hasegawa, J.; Ishida, M.; Nakajima, T.; Honda, Y.; Kitao, O.; Nakai, H.; Klene, M.; Li, X.; Knox, J. E.; Hratchian, H. P.; Cross, J. B.; Bakken, V.; Adamo, C.; Jaramillo, J.; Gomperts, R.; Stratmann, R. E.; Yazyev, O.; Austin, A. J.; Cammi, R.; Pomelli, C.; Ochterski, J. W.; Ayala, P. Y.; Morokuma, K.; Voth, G. A.; Salvador, P.; Dannenberg, J. J.; Zakrzewski, V. G.; Dapprich, S.; Daniels, A. D.; Strain, M. C.; Farkas, O.; Malick, D. K.; Rabuck, A. D.; Raghavachari, K.; Foresman, J. B.; Ortiz, J. V.; Cui, Q.; Baboul, A. G.; Clifford, S.; Cioslowski, J.; Stefanov, B. B.; Liu, G.; Liashenko, A.; Piskorz, P.; Komaromi, I.; Martin, R. L.; Fox, D. J.; Keith, T.; AlLaham, M. A.; Peng, C. Y.; Nanayakkara, A.; Challacombe, M.; Gill, P. M. W.; Johnson, B.; Chen, W.; Wong, M. W.; Gonzalez, C.; Pople, J. A. Gaussian 03, revision C.02; Gaussian, Inc.: Wallingford, CT, 2004.
- (19) Lindahl, E.; Hess, B.; van der Spoel, D. GROMACS 3.0: a package for molecular simulation and trajectory analysis. *J. Mol. Model.* **2001**, *7*, 306–317.
- (20) Darden, T.; York, D.; Pedersen, L. Particle mesh Ewald: An $N \cdot \log(N)$ method for Ewald sums in large systems. *J. Chem. Phys.* **1993**, *98*, 10089–10092.
- (21) Berendsen, H. J. C.; Postma, J. P. M.; Vangunsteren, W. F.; Dinola, A.; Haak, J. R. Molecular dynamics with coupling to an external bath. *J. Chem. Phys.* **1984**, *81*, 3684–3690.
- (22) Evrard, G.; Pusztai, L. Data versus constraints in reverse Monte Carlo modelling: a case study on molecular liquid CCl₄. *J. Phys.: Condens. Matter* **2005**, *17*, S37–S46.
- (23) Gereben, O.; Jovari, P.; Temleitner, L.; Pusztai, L. A new version of the RMC++ Reverse Monte Carlo programme, aimed at investigating the structure of covalent glasses. *J. Optoelectron. Adv. Mater.* **2007**, *9*, 3021–3027.
- (24) McGreevy, R. L. Reverse Monte Carlo modelling. *J. Phys.: Condens. Matter* **2001**, *13*, R877–R913.
- (25) Harsanyi, I.; Pusztai, L.; Soetens, J. C.; Bopp, P. A. Molecular dynamics simulations of aqueous RbBr-solutions over the entire solubility range at room temperature. *J. Mol. Liq.* **2006**, *129*, 80–85.
- (26) Soper, A. K. Joint structure refinement of x-ray and neutron diffraction data on disordered materials: application to liquid water. *J. Phys.: Condens. Matter* **2007**, *19*, 18.
- (27) Pusztai, L.; Pizio, O.; Sokolowski, S. Comparison of interaction potentials of liquid water with respect to their consistency with neutron diffraction data of pure heavy water. *J. Chem. Phys.* **2008**, *129*, 184103.
- (28) Keen, D. A. A comparison of various commonly used correlation functions for describing total scattering. *J. Appl. Crystallogr.* **2001**, *34*, 72–177.
- (29) Megyes, T.; Balint, S.; Grosz, T.; Radnai, T.; Bako, I.; Sipos, P. The structure of aqueous sodium hydroxide solutions: A combined solution x-ray diffraction and simulation study. *J. Chem. Phys.* **2008**, *128*, 12.
- (30) Aziz, E. F.; Ottosson, N.; Faubel, M.; Hertel, I. V.; Winter, B. Interaction between liquid water and hydroxide revealed by core-hole de-excitation. *Nature* **2008**, *455*, 89–91.
- (31) Smiechowski, M.; Stangret, J. Hydroxide ion hydration in aqueous solutions. *J. Phys. Chem. A* **2007**, *111*, 2889–2897.
- (32) Tuckerman, M. E.; Marx, D.; Parrinello, M. The nature and transport mechanism of hydrated hydroxide ions in aqueous solution. *Nature* **2002**, *417*, 925–929.